The $\alpha_2\delta$ subunit augments functional expression and modifies the pharmacology of Ca$_V$1.3 L-type channels

Arturo Andrade [a,1], Alejandro Sandoval [b,c], Ricardo González-Ramírez [b], Diane Lipscombe [d], Kevin P. Campbell [e], Ricardo Felix [b,*]

[a] Department of Physiology, Biophysics and Neuroscience, Center for Research and Advanced Studies of the National Polytechnic Institute, Cinvestav-IPN, Mexico City, Mexico
[b] Department of Cell Biology, Cinvestav-IPN, Mexico City, Mexico
[c] School of Medicine FES Iztacala, National Autonomous University of Mexico, Tlalnepantla, Mexico
[d] Department of Neuroscience, Brown University, Providence, RI, USA
[e] Howard Hughes Medical Institute and Department of Molecular Physiology and Biophysics, University of Iowa Roy J. and Lucille A. Carver College of Medicine, Iowa City, IA, USA

ARTICLE INFO

ABSTRACT

The auxiliary Ca$_V\alpha_2\delta$-1 subunit is an important component of voltage-gated Ca^{2+} (Ca$_V$) channel complexes in many tissues and of great interest as a drug target. Nevertheless, its exact role in specific cell functions is still unknown. This is particularly important in the case of the neuronal L-type Ca$_V$ channels where these proteins play a key role in the secretion of neurotransmitters and hormones, gene expression, and the activation of other ion channels. Therefore, using a combined approach of patch-clamp recordings and molecular biology, we studied the role of the Ca$_V\alpha_2\delta$-1 subunit on the functional expression and the pharmacology of recombinant L-type Ca$_V$1.3 channels in HEK-293 cells. Co-expression of Ca$_V\alpha_2\delta$-1 significantly increased macroscopic currents and conferred the Ca$_V$1.3α_1/Ca$_V\beta_3$ channels sensitivity to the antiepileptic/analgesic drugs gabapentin and AdGABA. In contrast, Ca$_V\alpha_2\delta$-1 subunits harboring point mutations in *N*-glycosylation consensus sequences or the proteolytic site as well as in conserved cysteines in the transmembrane δ domain of the protein, reduced functionality in terms of enhancement of Ca$_V$1.3α_1/Ca$_V\beta_3$ currents. In addition, co-expression of the δ domain drastically inhibited macroscopic currents through recombinant Ca$_V$1.3 channels possibly by affecting channel synthesis. Together these results provide several lines of evidence that the Ca$_V\alpha_2\delta$-1 auxiliary subunit may interact with Ca$_V$1.3 channels and regulate their functional expression.

© 2009 Elsevier Ltd. All rights reserved.

1. Introduction

L-type voltage-gated Ca^{2+} (Ca$_V$) channels are expressed in many different cell types and tissues. In myocytes they are essential for excitation–contraction coupling, whereas in neurons and endocrine cells they regulate neurotransmitter and hormone release, gene expression, and the activity of other ion channels [1,2]. Biochemical evidence suggests that L-type Ca$_V$ channels are comprised of five subunits. A principal transmembrane α_1 subunit is predicted to associate with a disulfide-linked $\alpha_2\delta$ dimer, an intracellular β subunit, and a transmembrane γ subunit [2,3]. The α_1 subunit is the ion-conducting element in the channel protein complex [2,3].

Four mammalian genes encode L-type Ca$_V$ channel α_1 subunits: Ca$_V$1.1 (also known as α_{1S}), Ca$_V$1.2 (α_{1C}), Ca$_V$1.3 (α_{1D}), and Ca$_V$1.4 (α_{1F}). Ca$_V$1.1α_1 and Ca$_V$1.4α_1 subunits are enriched in skeletal muscle and retina, respectively, whereas Ca$_V$1.2α_1 and Ca$_V$1.3α_1 subunits are expressed in many cells including neurons and endocrine cells [1,2]. Ca$_V$1.2 and Ca$_V$1.3 channels underlie the majority of L-type currents in neuronal, endocrine, and cardiovascular systems. Ca$_V$1.3 channels have relatively low activation thresholds, are less sensitive to dihydropyridine antagonists, and activate with fast kinetics when compared to Ca$_V$1.2 L-type currents [1]. There is growing interest in Ca$_V$1.2 and Ca$_V$1.3 channels because of their link to neurodegenerative disorders including autism, bipolar disorder, and Parkinson's disease [4–8]. Understanding the mechanisms that regulate L-type calcium channel activity and surface expression is of major importance.

In the central nervous system, L-type Ca^{2+} channels (Ca$_V$1.2 and Ca$_V$1.3) apparently do not support synaptic transmission, but seem to play an important role in the excitation–transcription coupling. It has been reported that Ca^{2+} entry via postsynaptic L-type channels activates transcription factors pCREB [9,10] and NFATc4

* Corresponding author at: Departamento de Biología Celular, Cinvestav-IPN, Avenida IPN #2508, Colonia Zacatenco, México D.F., CP 07300, Mexico.
Tel.: +52 55 50 61 39 88; fax: +52 55 50 61 33 93.
E-mail address: rfelix@fisio.cinvestav.mx (R. Felix).
[1] Present address: Department of Neuroscience, Brown University, Providence, RI, USA.

[11]. Phosphorylation of CREB, acting in conjunction with nuclear translocation and co-activator proteins promotes transcription of multiple genes [12,13]. Likewise, Ca$_V$1.3 channels play a unique role for hearing. Inner hair cells (IHCs), the primary sensory receptors of the mature mammalian cochlea, are responsible for relaying acoustic information transduced by mechano-sensitive channels to the central nervous system via afferent auditory nerve fibres. This is driven by Ca^{2+} entering IHCs through L-type channels of the Ca$_V$1.3 class [14] activated in response to depolarizing receptor potentials initiated by hair bundle deflection. In addition, it has been reported that Ca$_V$1.3 L-type channels are important for the sinoatrial node function. Using gene-targeted deletion of the Ca$_V$1.3α_1 subunit, Zhang et al. [15] found a decrease in the rate of firing associated with a diminished rate of diastolic depolarization. Last, Ca$_V$1.3 L-type channels are expressed at high density and play a role in the control of hormone secretion in a variety of endocrine cells including pancreatic β- and adrenal chromaffin cells where they control insulin and catecholamine release [2,16].

In contrast to the functional studies, the molecular architecture of the L-type Ca$_V$1.3 channels is largely unknown. Though a role for the Ca$_V\beta$ subunits in determining a functional interaction with protein kinase A [17] and arachidonic acid [18] has been reported, little is known regarding the role of the Ca^{2+} channel auxiliary subunits in the regulation of the Ca$_V$1.3 channel activity. On the other hand, it has been reported that Ca$_V\alpha_2\delta$ promotes surface expression of different Ca$_V\alpha_1$ subunits and it speeds channel activation and inactivation kinetics [19–30]. However, investigations of the Ca$_V\alpha_2\delta$ subunit effects on Ca$_V$1.3 channels are lacking. Here, we show that Ca$_V\alpha_2\delta$ augments surface expression of recombinant Ca$_V$1.3 channels in HEK-293 cells. We also show that co-expression of the Ca$_V\alpha_2\delta$ subunit renders the Ca$_V$1.3 channels sensitive to antiepileptic/analgesic gabapentinoid drugs (GBP and AdGABA) and that co-expression of the transmembrane δ domain alone, together with the Ca$_V$1.3/Ca$_V\beta_3$ Ca^{2+} channel combination in absence or presence of Ca$_V\alpha_2\delta$, results in an important inhibition of the whole-cell current.

2. Materials and methods

2.1. Materials

Chloroquine (C-6628) and Fillipin III (F-4767) were obtained from Sigma–Aldrich (St. Louis, MO) and prepared as stock according to the manufacturer's instructions. Gabapentin (1-(aminomethyl) cyclohexane acetic acid; Neurontin®; Pfizer; New York, NY) and AdGABA (a generous gift of Drs. G. Zoidis and N. Kolocouris, University of Athens) were prepared as stock in distilled water and aliquots were store at −20 °C. All other chemicals were of reagent grade and obtained from different commercial sources.

2.2. cDNA clones

Cell expression constructs were made by standard techniques and their fidelity was verified by DNA sequencing. The rat neuronal Ca$_V$1.3α_1 (GenBank accession number AF370009 [31]) was cloned into the pcDNA6/His vector (Invitrogen; Carlsbad, CA). The rabbit Ca$_V\beta_{1a}$ subunit (M25817) was cloned in the pKCRH$_2$ vector [32] while the cDNAs coding the rat brain Ca$_V\beta_{2a}$ (M80545), Ca$_V\beta_3$ (M88751) and Ca$_V\beta_4$ (L02315) subunits were cloned into the pcDNA3 vector (Invitrogen). We also used the recombinant bicistronic expression plasmid PIRES/$\alpha_2\delta$ [33], which carried the entire protein-coding region for the rat brain Ca$_V\alpha_2\delta$-1b Ca^{2+} channel auxiliary subunit (M86621), or its mutant constructs [27,33], and for the green fluorescent protein (GFP) coupled by an internal ribosomal entry site (IRES) sequence. The cDNA coding the Ca$_V\delta$

subunit, which was made by assembling a PCR fragment after the Ca$_V\alpha_2\delta$-1b signal sequence [22], and the CD8 surface marker were cloned in the pcDNA3 expression plasmid (Invitrogen). The PERK mutant constructs [34] were cloned into the pcDNAI/Amp vector (Invitrogen).

2.3. Site-directed mutagenesis

The Pfu DNA polymerase was used in all PCRs to generate the Ca$_V\alpha_2\delta$-1 mutations and all constructs were verified by sequencing. The glycosylation and proteolysis mutant constructs were generated following standard procedures in use in the laboratory [27,33]. The Ca$_V\alpha_2\delta$-1 subunit in which all cysteines in the extracellular region of δ were mutated to serines, was made using the pIRES-hrGFP-1a-based construct encoding the rat Ca$_V\alpha_2\delta$-1 [27] as a template and standard PCR techniques. In all cases, the mutations were introduced with 40-mer synthetic oligonucleotides using the Quick-Change XL II mutagenesis kit (Stratagene).

2.4. Cell culture and transfection

Human embryonic kidney (HEK)-293 cells (American Type Culture Collection, ATCC; Manassas, VA) were grown in Dulbecco's modified Eagle's medium (DMEM)-high glucose supplemented with 10% horse serum, 2 mM L-glutamine, 110 mg/l sodium pyruvate, 100 U/ml penicillin and 100 μg/ml streptomycin at 37 °C in a 5% CO$_2$/95% air humidified atmosphere. After splitting on the previous day and seeding at ~60% confluence, cells were transfected with the cDNA clones mentioned earlier using the Lipofectamine Plus reagent (Invitrogen) according to the manufacturer's instructions. After DNA–lipid complexes were allowed to form, cells were transfected with either cDNAs encoding Ca$_V$1.3α_1 alone (1 μg DNA/35-mm culture dish) or co-transfected with cDNAs for Ca$_V\beta$, Ca$_V\alpha_2\delta$-1 and Ca$_V\delta$ subunits in a 1:1 molar ratio (except where indicated).

The HEK-293 cell line stably expressing the Ca$_V$3.2 channel (GenBank accession number AF051946 [35]) was grown as previously described [36]. Likewise, the RIN-m5F insulinoma β-cells (ATCC) were cultured in RPMI-1620 medium supplemented with 10% fetal bovine serum, 100 U/ml penicillin and 100 μg/ml streptomycin. Both cell lines were plated on poly-L-lysine (0.05%)-precoated glass coverslips placed into 35-mm culture plates, and 24 h later were transfected with the Ca$_V\alpha_2\delta$-1 or δ subunit cDNA constructs using Lipofectamine Plus reagent (Invitrogen). 48 h after transfection, cells were subjected to electrophysiological recording.

2.5. Electrophysiology

Ionic currents were recorded using the whole-cell configuration of the patch-clamp technique [37], using an Axopatch 200B patch-clamp amplifier (Molecular Devices, Foster City, CA) and acquired on-line using a Digidata 1320A interface with pClamp8 software (Molecular Devices) as described elsewhere [27,33]. The offset potential between the pipette and bath solutions was zeroed prior to seal formation. After establishing the whole-cell mode, capacitive transients were cancelled with the amplifier. Series resistance values were typically 2–10 MΩ, and no records were used in which the voltage error (as defined by $V_{er} = I_{max} \times R_a$) was greater than 5 mV. Leak and residual capacitance currents were subtracted on-line by a P/4 protocol. Current signals were filtered at 2 kHz (internal 4 pole Bessel filter) and digitized at 5.71 kHz. Membrane capacitance (C_m) was determined as described previously [38] and used to normalize currents. The recording solutions are given in Table 1. Experiments were performed at room temperature (~22 °C).

Table 1
Recording solutions. Units are in mM. The pH was adjusted to 7.3 with KOH (A–C) and CsOH (D and E).

Sols	BaCl$_2$	CaCl$_2$	TEA-Cl	NaCl	CsCl	MgCl$_2$	KCl	K-Asp	HEPES	EGTA	Glucose	Na-ATP	Na-GTP
A	5		125						10		15		
B		5	125						10		15		
C		5		140			3		10		5		
D					140	5			10	10		4	0.1
E					0.2		8	130		10	10	5	

2.6. Semi-quantitative Western blot

Cells were mechanically detached from culture dishes, washed twice with PBS pH 7.4 (137 mM NaCl, 2.7 mM KCl, 10.1 mM Na$_2$HPO4, 1.8 mM KH$_2$PO$_4$) and lysed in triple-detergent buffer containing proteases inhibitors (50 mM Tris–HCl pH 8.0, 150 mM NaCl, 0.1% SDS, 1.0% NP-40, 0.5% sodium deoxycholate, 1 mM PMSF, complete 1X; Roche Diagnostics). Lysis was performed in ice for 20 min vortexing each 5 min. The extracts were centrifuged to remove insoluble debris (10 min: 7500 × g) and protein concentration in the supernatants was determined using Bradford assays. Samples with 50 μg of protein were boiled for 5 min in protein loading buffer (50 mM Tris–HCl [pH 6.8], 2% SDS, 10% glycerol, 5% β-mercaptoethanol, 0.01% bromophenol blue). Proteins were resolved in 10% SDS-polyacrylamide gels and transferred to nitrocellulose membranes (Amersham Biosciences; Piscataway, NJ). After blocking with 6% non-fat dry milk in TBS-T (10 mM Tris–HCl, 0.15 M NaCl, 0.05% Tween-20), membranes were incubated overnight with the primary anti-Ca$_V$1.3α$_1$ antibody (Alomone Labs; Jerusalem, Israel) (1:600 in blocking solution). Membranes were then washed and incubated with horseradish peroxidase goat anti-rabbit secondary antibody (Invitrogen) diluted in TBS-T with 6% non-fat dry milk and developed with the ECL reagent (Amersham Biosciences). For β$_3$, proteins were blotted onto nitrocellulose membranes and developed with enhanced chemiluminescence as previously described [22,39]. As a protein loading control, membranes were stripped and incubated with a mouse monoclonal anti-β-actin antibody [40].

Semi-quantitative analysis was carried out by densitometry using the Kodak digital Science ID v.2.0 system program.

2.7. Data analysis

Curve fitting and statistical analyses were carried out using the SigmaPlot 10 software package (SPSS Inc.; Chicago, IL). The significance of observed differences was evaluated by Student's unpaired t test. A probability less that 5% was considered to be significant. All experimental values are given as means ± S.E.M. The peak current values were converted to peak conductance values using the expression:

$$G = \frac{I}{(V_m - V_{rev})},\tag{1}$$

where I is current, G is conductance, V_m is the test potential and V_{rev} is the extrapolated reverse potential. Conductance–voltage (G–V) curves for activation were fit with a Boltzmann equation of the form:

$$G = \frac{G_{max}}{(1 + \exp[(V_m - V_{1/2})/k]^{-1}}\tag{2}$$

where G_{max} is maximum conductance, V_m is the test potential, $V_{1/2}$ is the potential for half-maximal activation of G_{max} and k is a slope factor.
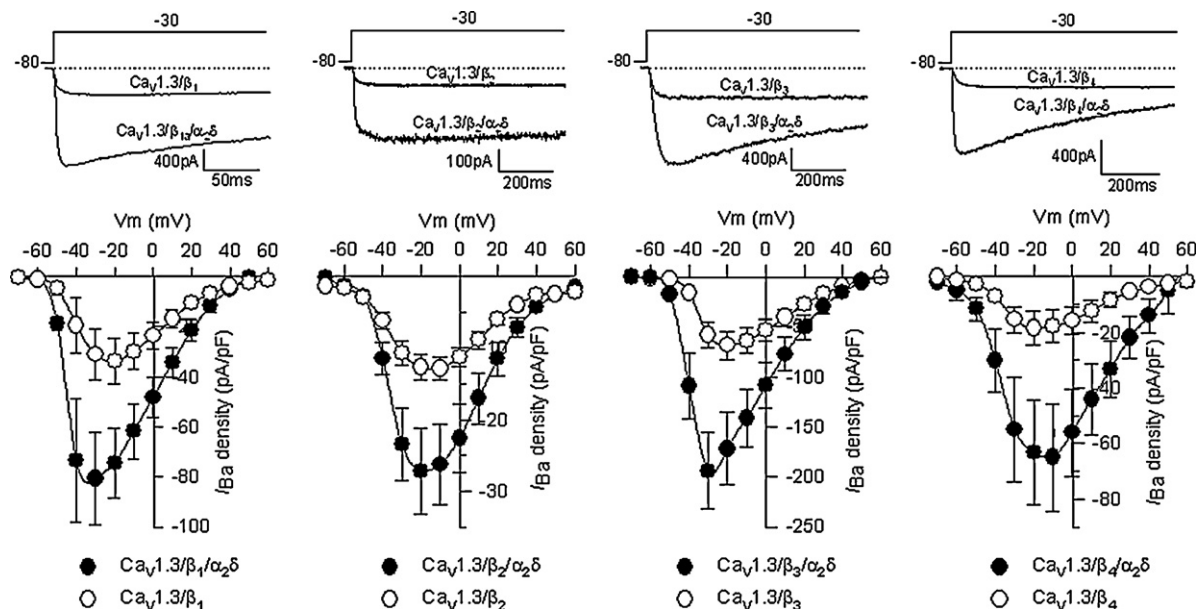
Fig. 1. Ca$_V$1.3 channel regulation by Ca$_V$β and Ca$_V$α$_2$δ-1 auxiliary subunits. The upper panels show representative traces of macroscopic Ba^{2+} current (I_{Ba}) recorded from HEK-293 cells that expressed Ca$_V$1.3 channels in association with the Ca$_V$β subunit (β$_{1a}$, β$_{2a}$, β$_3$ or β$_4$) in absence and presence of the Ca$_V$α$_2$δ-1 subunit, using solutions A (external) and D (internal) (Table 1). Currents were elicited by a depolarizing pulse to −30 mV from a V_h of −80 mV. The lower panels show average I–V relationships for I_{Ba} recorded from cells expressing Ca$_V$1.3α$_1$/β channels in absence and presence of the Ca$_V$α$_2$δ-1 subunit (n = 9–50 cells). Currents were evoked by 10-mV depolarizing steps from a V_h of −80 mV to potentials between −70 and +60 mV.
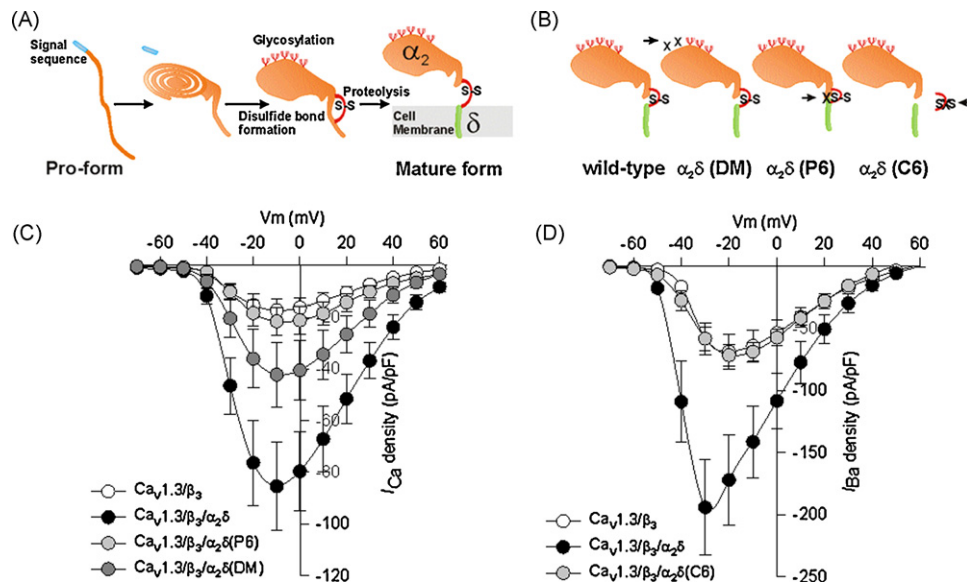
Fig. 2. $Ca_V\alpha_2\delta$-1 mutant subunits are unable to increase current amplitude through $Ca_V1.3\alpha_1/\beta_3$ channels. (A) The $Ca_V\alpha_2\delta$-1 subunit is synthesized in the endoplasmic reticulum as a pro-form that consists of a signal sequence, the α_2 and the δ domains, and its post-translational processing includes the removal of the signal sequence, glycosylation of the α_2 domain and disulfide bond formation between α_2 y δ and proteolytical cleavage to acquire its mature form. (B) Three different $Ca_V\alpha_2\delta$-1 mutant subunits were used in this work: $\alpha_2\delta$ (DM) has two point mutations in N-glycosylation sites; $\alpha_2\delta$ (P6) has a mutation in the putative site of proteolytic processing and a construct lacking the conserved cysteines of the extracellular region of δ (C6). (C) Average I–V relationships for I_{Ca} recorded from HEK-293 cells expressing $Ca_V1.3\alpha_1/\beta_3$ channels in presence of the wild-type $Ca_V\alpha_2\delta$-1 subunit or its mutant constructs P6 and DM. $n = 9$–18 recorded cells. (D) Average I–V relationships for I_{Ba} recorded from HEK-293 cells expressing $Ca_V1.3\alpha_1/\beta_3$ channels in presence of the wild-type $\alpha_2\delta$-1 or the $\alpha_2\delta$ (C6) construct. Currents were recorded using solutions B/D (panel A) and A/D (panel B), respectively (see Table 1), and were elicited by 10-mV depolarizing steps from a V_h of -80 mV to potentials between -70 and $+60$ mV ($n = 30$–60 recorded cells).

Steady-state inactivation curves were fitted with a Boltzmann function:

$$I = \frac{I_{\max}}{(1 + \exp[(V_m - V_{1/2})/k])}, \qquad (3)$$

where the current amplitude I has decreased to a half-amplitude at $V_{1/2}$ with an e-fold change over k mV.

Current activation and decay were fitted with a second order exponential equation of the form:

$$I = A_{\text{fast}} \exp\left(\frac{-t}{\tau_{\text{fast}}}\right) + A_{\text{slow}} \exp\left(\frac{-t}{\tau_{\text{slow}}}\right), \qquad (4)$$

where t represents the time after the onset of the test pulse, A_{fast} and A_{slow} are the contribution of a fast and a slow component to the total current amplitude, and τ_{fast} and τ_{slow} are the time constants associated with each component.

3. Results

3.1. The $Ca_V\alpha_2\delta$-1 subunit increases macroscopic Ca^{2+} currents in cells expressing recombinant $Ca_V1.3$ channels

We co-expressed $Ca_V\alpha_2\delta$-1 and $Ca_V1.3$ subunits together with different $Ca_V\beta$ subunits in HEK-293 cells to establish if $Ca_V\alpha_2\delta$-1 plays a role in regulating expression levels of $Ca_V1.3$ L-type channels. Ca^{2+} channel currents in cells expressing $Ca_V\alpha_2\delta$-1 were substantially greater (3–5-fold) than those in cells lacking exogenous $Ca_V\alpha_2\delta$-1. This effect of $Ca_V\alpha_2\delta$-1 occurred regardless of $Ca_V\beta$ subunit type and was independent of test voltage (Fig. 1). Given that Western blot experiments have shown that untransfected HEK-293 cells do not express endogenous $Ca_V\alpha_2\delta$-1 [33], $Ca_V1.3/Ca_V\beta$ current enhancement detected after transfection may be therefore considered to be mediated by the heterologously expressed $Ca_V\alpha_2\delta$-1 subunit. Likewise, our subsequent investigations of $Ca_V\alpha_2\delta$-1 focused on the $Ca_V1.3/Ca_V\beta_3$ combination because these two subunits tend to co-exist in neuronal and neuroendocrine tissue [41,42].
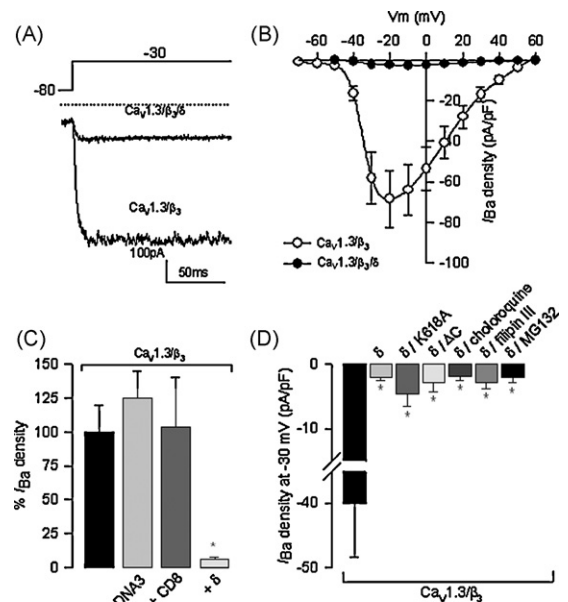
Fig. 3. The δ subunit inhibits the functional expression of $Ca_V1.3\alpha_1/\beta_3$ channels. (A) Representative traces of I_{Ba} recorded from HEK-293 cells expressing $Ca_V1.3\alpha_1/\beta_3$ channels in absence and presence of δ using solutions A and D (Table 1). Currents were elicited by a 140 ms depolarizing pulse to -30 mV from a V_h of -80 mV. (B) Average I–V relationships for I_{Ba} recorded from HEK-293 cells expressing $Ca_V1.3\alpha_1/\beta_3$ channels with or without δ. Currents were evoked by 10-mV depolarizing steps from a V_h of -80 mV to potentials between -70 and $+60$ mV. (C) Relative I_{Ba} densities obtained from cells expressing $Ca_V1.3\alpha_1/\beta_3$ channels alone (control; solid bar), plus the empty vector pcDNA3, the transmembrane protein CD8 or the δ subunit as listed. $n = 5$–18 recorded cells. (D) Mean I_{Ba} density obtained of HEK-293 cells expressing $Ca_V1.3\alpha_1/\beta_3$ channels in absence and presence of δ and after co-transfection with the PERK negative dominant construct cDNAs (K618A and ΔC), or after treatment with chloroquine (100 μM), filipin III (5 μg/ml) or MG-132 (25 μM). $n = 9$–31 recorded cells. The asterisk denotes significant differences ($p < 0.05$) respect to the control value.
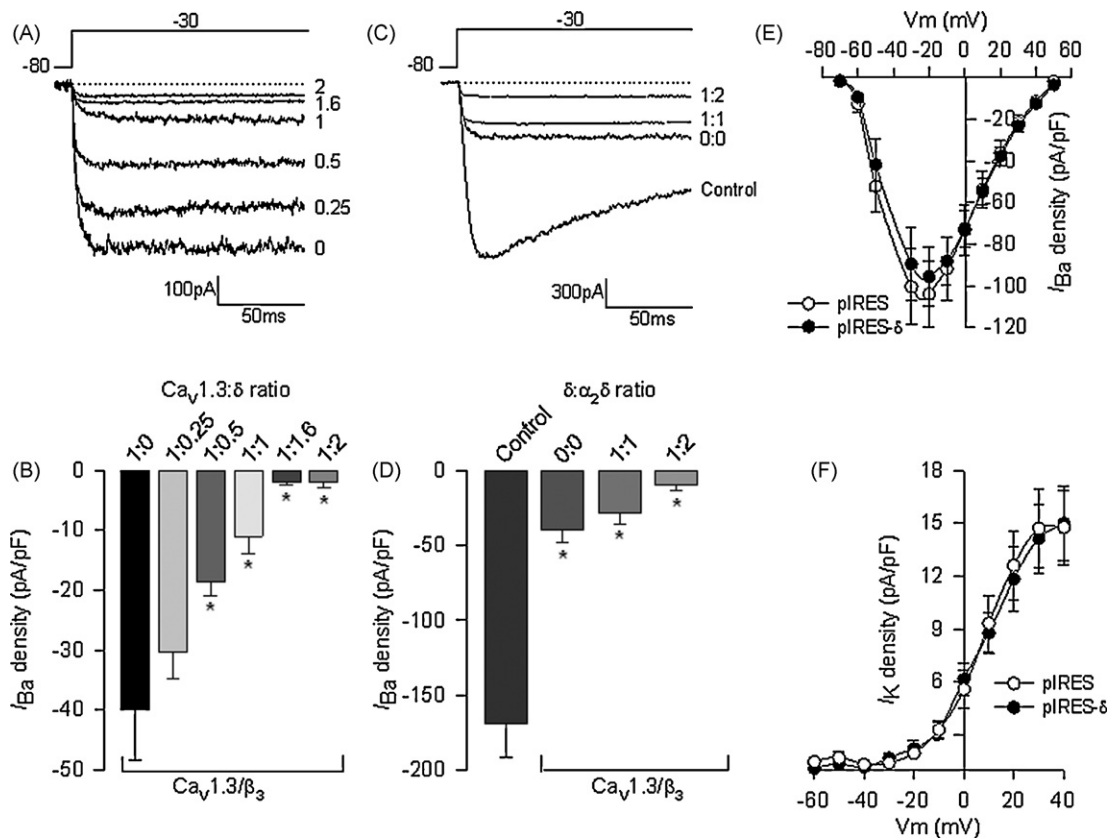
Fig. 4. The inhibitory actions of the δ subunit on recombinant $Ca_V1.3\alpha_1/\beta_3$ channel are specific. (A) Representative traces of I_{Ba} current evoked in HEK-293 cells expressing $Ca_V1.3\alpha_1/\beta_3$ channels, transfected with various concentrations of δ. Currents were elicited by depolarizing pulses to -30 mV from a V_h of -80 mV. (B) Comparison of I_{Ba} densities obtained in cells transfected with the different concentrations of the δ plasmid. Asterisks denote significant differences ($p < 0.05$) with respect to the control. $n = 8$–21 recorded cells. (C) Representative traces of I_{Ba} evoked in cells expressing $Ca_V1.3\alpha_1/Ca_V\beta_3/Ca_V\alpha_2\delta$-1 channels in absence and presence of δ in equal (1:1) or double molar relationship (2:1) with respect to the other channel subunits. Currents were evoked as in A. (D) Comparison of mean I_{Ba} density obtained of HEK-293 cells as in C. $n = 19$–60 recorded cells. Asterisks denote significant differences ($p < 0.05$) with respect to the control. (E) Average I–V relationships for I_{Ba} recorded from HEK-293 cells stably expressing $Ca_V3.2$ channels in absence (pIRES empty vector) and presence of δ cloned into the mammalian expression pIRES vector. Currents were elicited by 100 ms depolarizing pulses in 10 mV steps from a V_h of -80 mV. (B) Average I–V relationships for macroscopic endogenous K$^+$ currents (I_K) recorded from HEK-293 cells in absence (pIRES empty vector) and presence of δ using solutions C and E (Table 1). Currents were elicited by 200 ms depolarizing pulses in 10 mV steps from a V_h of -80 mV ($n = 10$–14 cells).

We next used more physiological recording conditions to test if $Ca_V\alpha_2\delta$-1 augmented $Ca_V1.3$ currents when calcium is the charge carrier (Supplemental Fig. 1). L-type currents recorded with Ca^{2+} inactivate during the test pulse because they undergo pronounced Ca^{2+}-dependent inactivation [43,44]. In cells expressing the $Ca_V\alpha_2\delta$-1 subunit, L-type currents exhibited more prominent Ca^{2+}-dependent inactivation at voltages > -40 mV reflecting greater levels of Ca^{2+} entry [45,46]. Under these recording conditions, $Ca_V\alpha_2\delta$-1 still increased L-type current density over a range of voltages and without affecting the voltage dependence of channel activation and steady-state inactivation.

3.2. Effect of over-expression of $Ca_V\alpha_2\delta$-1 mutant constructs on recombinant $Ca_V1.3\alpha_1/Ca_V\beta_3$ channels

We were interested in knowing if the stimulatory effects of $Ca_V\alpha_2\delta$-1 on $Ca_V1.3$ channels are similar to its reported effects on $Ca_V2.2$. As mentioned earlier, $Ca_V\alpha_2\delta$-1 is a glycosylated polypeptide that possesses a single transmembrane domain (δ) with a short intracellular C terminus and a long extracellular portion (Fig. 2A) which serves as an anchor in the cell membrane [2,3,47]. We know that N-glycosylation at N136 and N184 and proteolytic processing at amino acid residues 941–946 of $Ca_V\alpha_2\delta$-1 are important for its stimulatory effects on neuronal $Ca_V2.2$ channels [27,33]. We therefore asked if the same sites play a role in $Ca_V\alpha_2\delta$-1 mediated stimulation of $Ca_V1.3$ channels using different mutant constructs

(Fig. 2B). As can be seen in Fig. 2C, the stimulatory effects of $Ca_V\alpha_2\delta$-1 were partially lost in the double N-glycosylation $Ca_V\alpha_2\delta$-1 mutant, N136Q and N184Q [33], and completely abolished in the proteolytic-site truncated $Ca_V\alpha_2\delta$-1 mutant, P6 [27]. It is worth noting that previous results in our laboratory indicate that both mutant constructs are expressed in the HEK-293 cells at similar levels than the wild-type $Ca_V\alpha_2\delta$-1 protein [27,33].

We also tested a $Ca_V\alpha_2\delta$-1 construct in which we mutated all six conserved cysteine residues in the δ domain (C6), to prevent association with α_2. The C6 $Ca_V\alpha_2\delta$-1 mutant was also unable to augment $Ca_V1.3$ channel currents (Fig. 2D) implying that association between α_2 and δ subunits is needed for its effects on current density. As with the double N-glycosylation and proteolytic-site mutated versions of $Ca_V\alpha_2\delta$-1, the C6 mutant is not express at a significantly different level than wild-type in the HEK-293 cells (data not shown).

3.3. The δ domain attenuates $Ca_V1.3\alpha_1/Ca_V\beta_3$ channel expression

Although the actions of the $Ca_V\alpha_2\delta$-1 subunit have been probed using various glycosylation and deletion mutants, the effect of the δ domain in isolation from α_2 is still virtually unexplored [22,48]. We therefore assessed the effect of the δ domain on $Ca_V1.3$ channel currents. L-type currents in cells expressing the δ subunit were significantly smaller compared to currents in control cells over a range of test voltages (Fig. 3A and B). We also compared currents in
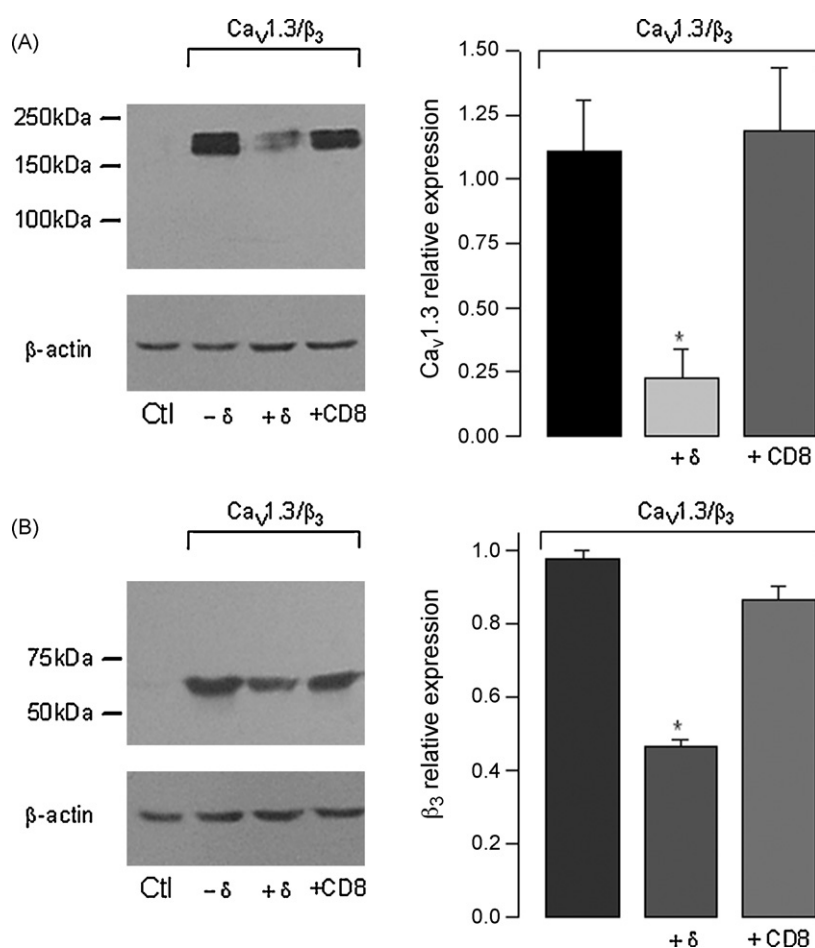
Fig. 5. δ domain-induced inhibition is related to decreased Ca_V subunits expression. (A) The left panel shows the Western blot analysis of membranes from untransfected HEK-293 cells (lane 1) or cells expressing $Ca_V1.3\alpha_1$/$Ca_V\beta_3$ channels (lane 2) in presence of the δ domain (lane 3) or the transmembrane protein CD8 (lane 4), using an antibody that recognizes the $Ca_V1.3\alpha_1$ protein. A ~200 kDa band, the expected molecular mass of rat $Ca_V1.3\alpha_1$ is detected in cells expressing recombinant $Ca_V1.3\alpha_1$/$Ca_V\beta_3$ channels both in presence and absence of δ. The right panel shows a densitometric analysis of the bands. (B) The left panel shows the Western blot analysis of membranes from HEK-293 cells as in (A) using an antibody that recognizes the $Ca_V\beta_3$ protein (~60 kDa). The right panel shows a densitometric analysis of the bands. In both cases bars represent averaged data (±S.E.M.) from three independent experiments; the relative levels of the $Ca_V1.3\alpha_1$ and the $Ca_V\beta_3$ protein expression were analyzed after normalization to those of β-actin. Mean values for the cells that did not express δ were set at 100%.

cells co-expressing δ with those lacking δ and those expressing an unrelated control protein CD-8 (Fig. 3C). Likewise, we found that the inhibitory effects of δ were independent of recording conditions and observed when Ca^{2+} or Ba^{2+} were used as charge carriers (Supplemental Fig. 2).

The effects of δ reported here may be the result of a long-term regulation. It is possible that the $Ca_V\delta$ subunit affect processes that control surface targeting and/or overall levels of $Ca_V1.3$ protein. To test if the inhibitory effects of δ involved internalization, we used chloroquine, a lysosomal inhibitor, filipin III, a raft/caveolae-dependent endocytosis inhibitor and MG-132, a selective inhibitor of the 26S proteasome. Neither internalization inhibitor interfered with the actions of δ on L-type current density (Fig. 3D).

The inhibitory effects of the δ domain on current density depended on cDNA concentrations. Using fixed levels of $Ca_V1.3\alpha_1$ and $Ca_V\beta_3$ cDNAs (1:1 molar ratio) we varied δ cDNA levels and show a dose dependent decrease in L-type current densities with an increase in the relative molar ratio of δ (Fig. 4A and B). Interestingly, wild-type $Ca_V\alpha_2\delta$-1 could not compete away the inhibitory effects of δ (Fig. 4C and D). L-type currents measured in cells co-expressing ($Ca_V1.3\alpha_1$/$Ca_V\beta_3$/$Ca_V\alpha_2\delta$) were attenuated greatly in the presence of δ, suggesting a possible interaction of δ with the channel complex. Likewise, the inhibitory action of δ was channel specific inhibiting $Ca_V2.2$ (Supplemental Fig. 3) and $Ca_V1.3$

channels (Fig. 4A–C) but not affecting low voltage-activated $Ca_V3.2$ (T-type) currents or endogenous K^+ currents recorded in untransfected HEK-293 cells (Fig. 4E and F).

3.4. δ Decreases $Ca_V1.3$ channel expression

We next quantified the levels of $Ca_V1.3\alpha_1$ and $Ca_V\beta_3$ subunits in cells expressing and lacking δ by Western blotting using $Ca_V1.3$ and $Ca_V\beta_3$ specific antibodies. Levels of both $Ca_V1.3\alpha_1$ and $Ca_V\beta_3$ subunits, but not control CD8 protein were significantly lower in cells expressing δ compared to control cells (Fig. 5). The δ-dependent decrease in $Ca_V1.3$ and $Ca_V\beta_3$ protein levels might not involve the unfolded protein response (UPR) pathway which has been implicated in the mechanism of action of hemi-Ca^{2+} channels and Ca^{2+} channel-related subunits [49–51], given that two mutant kinase-lacking PERK constructs, PERK ΔC and PERK K618A [34], that interfere with this pathway apparently did not prevent the inhibitory effects of δ on $Ca_V1.3$ L-type currents (Fig. 3D).

3.5. Native L-type current are regulated by wild-type $\alpha_2\delta$-1 and isolated δ subunits

We next asked if $Ca_V\alpha_2\delta$-1 could also influence native $Ca_V1.3$ L-type channels and used RIN-m5F rat insulinoma β-cells. Transient
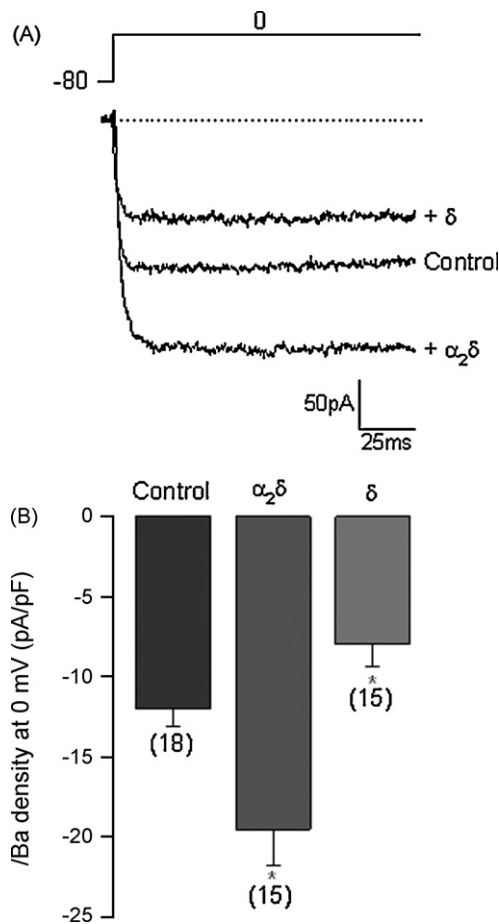
Fig. 6. The $\alpha_2\delta$-1 subunit regulates native L-type Ca_V channels in RIN-m5F cells. (A) Representative traces of native I_{Ba} recorded from rat insulinoma RIN-m5F cells mock transfected with the pIRES empty vector (control), or the cDNAs coding for the $Ca_V\alpha_2\delta$-1 subunit or the δ domain. Currents were elicited by voltage steps to 0 mV from a V_h of −80 mV using solutions A and D (Table 1). (B) Mean I_{Ba} density obtained from RIN-m5F control cells and in presence of the $Ca_V\alpha_2\delta$-1 or the δ constructs as in (A). The asterisk denotes significant difference ($p < 0.05$). The number of recorded cells is indicated in parentheses.

expression of exogenous wild-type $Ca_V\alpha_2\delta$-1 and δ in RIN-m5F cells resulted in significantly larger and smaller currents densities, respectively, when compared to control L-type currents supporting a role for $Ca_V\alpha_2\delta$-1 in controlling overall activity of $Ca_V1.3$ L-type channels (Fig. 6).

Although the role of the $Ca_V\gamma$ subunit as a component of neuronal Ca_V channels is still a matter of debate [51,52], we considered important to examine whether the actions of $Ca_V\gamma$ could alter the inhibitory effect of $Ca_V\delta$. To this end, we performed Western blot experiments in the RIN-m5F cell line to investigate if $Ca_V\gamma_2$ was expressed. The result of this analysis indicates that the $Ca_V\gamma$ auxiliary subunit is absent in these cells (Supplemental Fig. 4). Given that the macroscopic Ca^{2+} currents in the RIN-m5F cells are indeed affected by $Ca_V\delta$ expression, it is reasonable to conclude that this inhibition is independent of $Ca_V\gamma$.

3.6. $Ca_V\alpha_2\delta$-1 modifies the pharmacology of $Ca_V1.3$ L-type channels

The $Ca_V\alpha_2\delta$ subunit modifies the pharmacological sensitivity of neuronal Ca^{2+} channels to drugs. Most notable, gabapentin (GBP) inhibits N- and P/Q-type channels but only when they associate with $Ca_V\alpha_2\delta$-1 and $Ca_V\alpha_2\delta$-2 [30,53–55]. There is evidence that

the $Ca_V\alpha_2\delta$-dependent inhibitory actions of GBP and its analogs are important for its therapeutically beneficial actions as analgesics [56]. We were therefore interested in knowing if $Ca_V\alpha_2\delta$-1 could also modify the pharmacological sensitivity of $Ca_V1.3$ L-type currents to GBP. Chronic exposure (48 h) to 1 mM GBP, had a small effect on peak L-type current amplitudes in cells expressing $Ca_V1.3\alpha_1/Ca_V\beta_3$ with and without $Ca_V\alpha_2\delta$-1 (Fig. 7A). Average peak L-type current density at −10 mV was −89 ± 22 in absence and −85 ± 17 pA/pF in presence of the drug. However, in consistency with previous reports showing inhibition of recombinant N-type $Ca_V2.2$ channel activity [30,53], in our hands GBP strongly decreased $Ca_V2.2/Ca_V\beta_3$ current density when co-expressed with $Ca_V\alpha_2\delta$-1 (Fig. 8), suggesting differential responses of distinct channel types to the drug.

On the other hand, GBP did influence the voltage dependence of $Ca_V1.3\alpha_1/Ca_V\beta_3/Ca_V\alpha_2\delta$-1 channel activation as well as the kinetics of activation and inactivation. GBP induced ~10 mV right shift in the voltage dependence of L-channel activation, increased the rate of channel activation, and decreased the rate of the slow component of channel inactivation (Fig. 7B). The effect of GBP on the slow component of L-channel inactivation is consistent with its effects on other (N- and P/Q-type) Ca^{2+} channels [30,57].

Finally, we examined the effects of 2-aminomethyl-2-tricyclo[3.3.1.1^{1,7}]decaneacetic acid hydrochloride **5** (AdGABA), a novel adamantine derivative of GABA that also has strong inhibitory effects on recombinant N-type channels [54]. It is worth noting that although the pharmacological evaluation of AdGABA has demonstrated anticonvulsive and antinociceptive properties, these properties were detectable only at high (sedative) doses, which may limit its potential clinical use. However, both gabapentin (GBP) and AdGABA seem to be acting via the same mechanism [54].

Chronic exposure (48 h) to 1 mM AdGABA strongly inhibited peak L-type current amplitudes in cells expressing $Ca_V1.3\alpha_1/Ca_V\beta_3$ with $Ca_V\alpha_2\delta$-1 (~2.2-fold inhibition) but not in cells without $Ca_V\alpha_2\delta$-1 (Fig. 7C). AdGABA did not affect the voltage dependence or rate of channel activation but like GBP, it lengthened the slow component of channel inactivation in cells expressing $Ca_V\alpha_2\delta$-1 (Fig. 7D).

The pharmacological changes in $Ca_V1.3$ L-channels mediated by $Ca_V\alpha_2\delta$-1 are mechanistically similar to those on $Ca_V2.2$ N-type channels, but the channels differ in their pharmacological specificity for GBP and AdGABA. Preferential action on $Ca_V2.2$ channels by GBP (Fig. 8) might explain why this drug is an effective analgesic.

4. Discussion

Although neuronal L-type Ca^{2+} channels are thought to open too slowly to contribute to action potential-dependent Ca^{2+} entry, they seems to play an essential role in regulating activity-dependent gene expression. A complication of studying native L-type channels is that they represent a minor fraction of the whole-cell Ca^{2+} current in most neurons. A common approach to overcome this problem is the use of cellular systems over-expressing the $Ca_V1.3\alpha_1$ channel protein [31,41,58].

Diverse effects of the auxiliary $Ca_V\alpha_2\delta$-1 subunit have been reported on the properties of cloned high voltage-activated Ca^{2+} channels. Heterologous co-expression of this protein with neuronal $Ca_V2.1\alpha_1$ [25,48,59], $Ca_V2.2\alpha_1$ [27,33], $Ca_V2.3\alpha_1$ [25,60] or cardiac $Ca_V1.2\alpha_1$ [19,20,22,25,61,62] and various combinations of $Ca_V\beta$ subunits resulted in a significant increase in current amplitude. The $Ca_V\alpha_2\delta$-1 subunit has been also shown to mediate hyperpolarizing shifts in the voltage dependence of Ca^{2+} channel activation [25] and inactivation [19,22,25], in addition to regulating the kinetics of current activation [19,62] and inactivation [19,22,59]. The
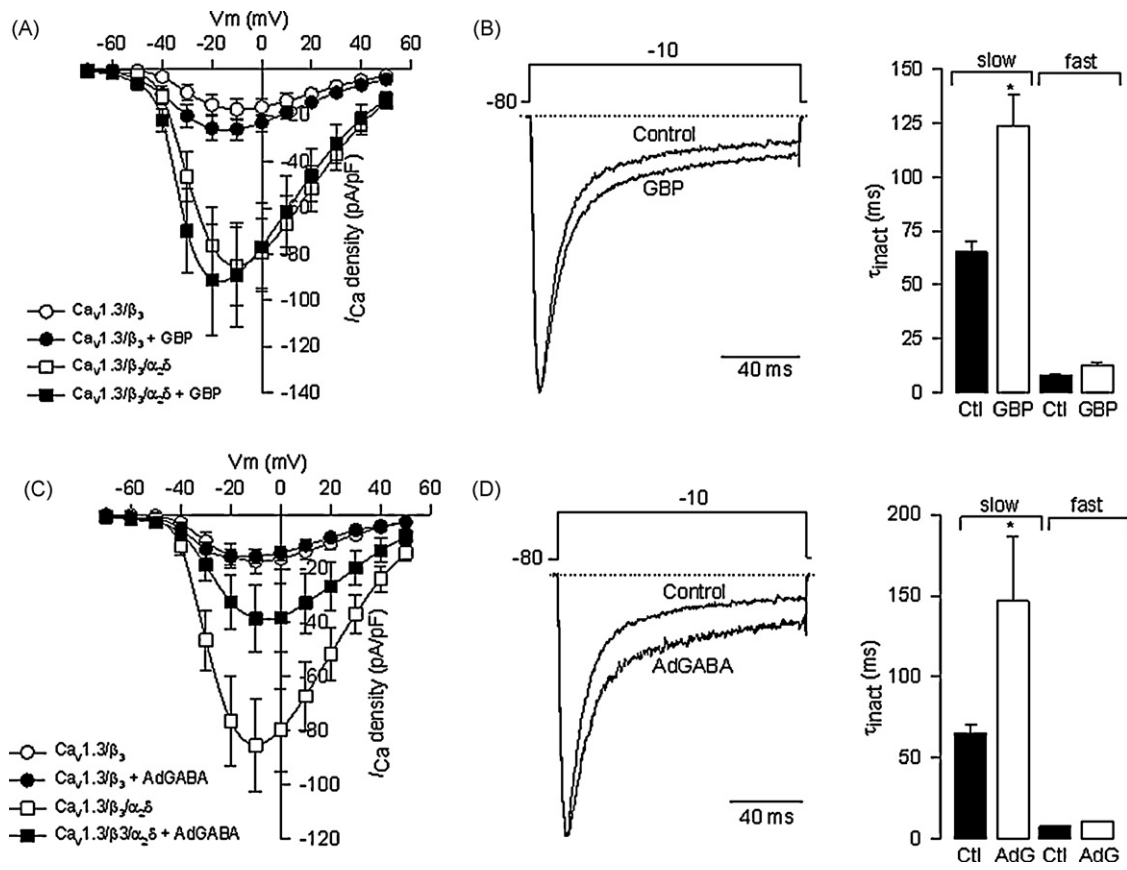
Fig. 7. The $\alpha_2\delta$-1 auxiliary subunit renders the Ca$_V$1.3α_1/β_3 channels sensitive to gabapentinoids. (A) Average I–V relationships for I_{Ca} recorded from HEK-293 cells expressing Ca$_V$1.3α_1/Ca$_V\beta_3$ channels, with or without Ca$_V\alpha_2\delta$-1, in absence and presence of 1 mM gabapentin (GBP) for 48 h. Currents were evoked by 10-mV depolarizing steps from a V_h of -80 mV to potentials between -70 and $+50$ mV. $n = 9$–22 recorded cells. (B) Superimposed normalized current traces in absence (control) and presence of the drug. Currents were elicited by a 140 ms depolarizing pulse to -10 mV from a V_h of -80 mV. (C) Comparison of slow and fast components of inactivation (τ_{inact}) in absence and presence of GBP. The values of τ_{inact} were obtained by fitting the decaying phase of current traces with Eq. (4). The asterisk denotes significant differences ($p < 0.05$) compared with control. (D) Average I–V relationships for I_{Ca} recorded from HEK-293 cells expressing Ca$_V$1.3α_1/Ca$_V\beta_3$ channels, with or without Ca$_V\alpha_2\delta$-1, in absence and presence of 1 mM AdGABA for 48 h. Currents were evoked by 10-mV depolarizing steps from a V_h of -80 mV to potentials between -70 and $+50$ mV. (E) Superimposed normalized typical current traces in absence (control) and presence of the drug. Currents were elicited by a 140 ms depolarizing pulse to -10 mV from a V_h of -80 mV. (F) Comparison of slow and fast components of inactivation (τ_{inact}) in absence and presence of AdGABA. The asterisk denotes significant difference ($p < 0.05$) compared with control ($n = 15$–17 cells).
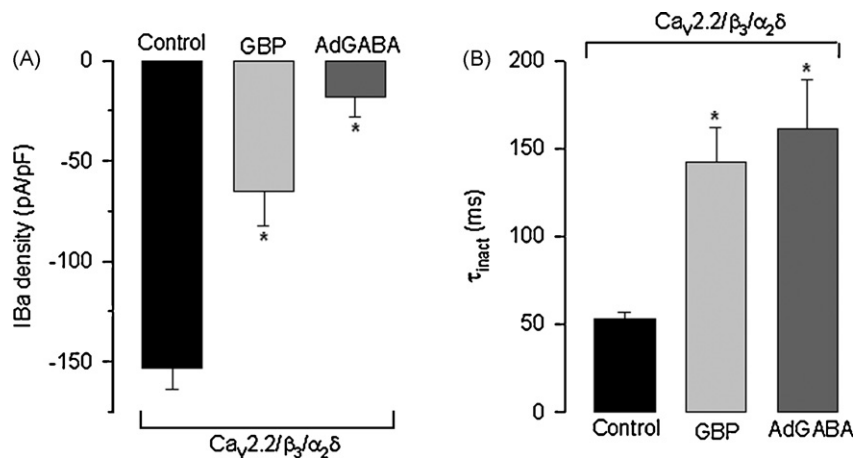
Fig. 8. Inhibition of recombinant N-type Ca$_V$ channels by gabapentinoids. (A) Mean I_{Ba} density obtained from HEK-293 cells expressing Ca$_V$2.2α_1/β_3/$\alpha_2\delta$-1 channels in the control condition and after chronic treatment (48 h) with 1 mM GBP or AdGABA using solutions A and D (Table 1). Currents were elicited by a 140 ms depolarizing pulse to $+10$ mV from a V_h of -80 mV. $n = 7$–17 recorded cells. (B) Comparison of the time constants of inactivation (τ_{inact}) in absence after the exposure to GBP and AdGABA as indicated. The values of τ_{inact} were obtained by fitting the decaying phase of current traces with Eq. (4). The asterisk denotes significant differences ($p < 0.05$) compared with control.

increase in current amplitude could be attributed to enhanced targeting of expressed $Ca_V\alpha_1$ subunits to the plasma membrane, while the effects on the time course and/or voltage dependence of current activation and inactivation suggest a more specific modulation of the channel's gating.

Very recently, the first successful attempt at knocking out the $Ca_V\alpha_2\delta$-1-subunit has been reported. A comparison of the electrophysiological properties in isolated cardiomyocytes from the $Ca_V\alpha_2\delta$-1 ($-/-$) and wild-type mice showed that the absence of the $Ca_V\alpha_2\delta$-1 gene results in an attenuated Ca^{2+} current amplitude, a decrease in Ca^{2+} density, an increase in the time constants (fast and slow), and a depolarizing shift in activation and inactivation [63]. Interestingly, the ablation of the $Ca_V\alpha_2\delta$-1 subunit resulted in reduced GBP binding in the knock-out animals compared with wild-type in either brain or skeletal muscle [63].

Likewise, recent studies have shown that the $Ca_V\alpha_2\delta$-1 subunit might play a more pronounced role in regulating current amplitudes than the other Ca^{2+} channel auxiliary subunits [25]. In spite of this, to date, there have been relatively few studies showing the effects of $Ca_V\alpha_2\delta$-1 on L-type $Ca_V1.3$ channel activity [41,64]. Indeed, it has not yet been investigated whether the expression of the $Ca_V1.3\alpha_1$ subunit requires this auxiliary subunit for trafficking to the cell membrane, or for functional expression, or whether $Ca_V\alpha_2\delta$-1 influences the biophysical properties of the $Ca_V1.3$ channels in mammalian cells. In the present study we show that co-expression of the $Ca_V\alpha_2\delta$-1 subunit has clear effects on the functional expression of recombinant and native $Ca_V1.3$ channels. Over-expression of exogenous $Ca_V\alpha_2\delta$-1 produced a ~3–5-fold increase in the amplitude of currents through recombinant $Ca_V1.3\alpha_1/Ca_V\beta_3$ channels expressed in HEK-293 cells, but had only minor effects on their kinetics or voltage dependence of activation and inactivation. Interestingly, similar effects have been previously reported in *Xenopus* oocytes in which the amplitude of neuroendocrine $Ca_V1.3\alpha_1/Ca_V\beta_3$ channel currents was increased by ~2–5-fold upon co-expression of the $Ca_V\alpha_2\delta$ subunit [41]. This argues either for an effect of the auxiliary subunit on the trafficking of the nascent $Ca_V1.3\alpha_1/Ca_V\beta_3$ channels from the endoplasmic reticulum to the cell membrane, or an effect to stabilize the membrane channels in a functional conformation. Further studies will be necessary to determine whether $Ca_V\alpha_2\delta$-1 affects the properties of the currents acting at the single channel level.

In order to evaluate in more detail the molecular determinants of $Ca_V1.3$ channel regulation by the $Ca_V\alpha_2\delta$-1 subunit, a series of site-directed mutants was constructed and functionally analyzed. The amino acids N136 and N184 as well as the sequence between residues R941 to V946 in the protein has been described previously to be important for the subunit-induced current stimulation [27,33]. The two asparagine residues seem to be glycosylated *in vivo* while the six amino acids localized between A941 and V946 (Arg-Leu-Leu-Glu-Ala-Val) presumably constitute the proteolytic site in $Ca_V\alpha_2\delta$-1. Substitution of such amino acids renders the $Ca_V\alpha_2\delta$-1 subunit non-functional as shown by patch-clamp experiments in experiments using $Ca_V2.2\alpha_1/Ca_V\beta_3$ channels. Consistent with this, electrophysiological recordings performed in cells expressing mutant constructs indicated that the stimulatory effect of $Ca_V\alpha_2\delta$-1 on macroscopic currents through $Ca_V1.3\alpha_1/Ca_V\beta_3$ channels was partially or completely lost. Last, the same experiments were repeated for a construct in which all cysteine residues in the extracellular region of δ were substituted by methionine or serine (C962M; C984S; C987S; C1032S; C1047S; C1059S). Mutation of the six residues also abolished the stimulatory effect of $Ca_V\alpha_2\delta$-1 on functional $Ca_V1.3\alpha_1/Ca_V\beta_3$ channels, suggesting that the disulphide linkage between the α_2 and the δ polypeptides is required for function. Given that the voltage dependence and time course for the activation and inactivation of the channels were practically unaltered, these effects of the $Ca_V\alpha_2\delta$-1 mutant constructs may not be explained by alterations in the functional properties of the channels, but might involve a reduced number of functional channels in the surface of the membrane.

Another interesting finding of our study was that the δ domain of the $Ca_V\alpha_2\delta$-1 auxiliary subunit exerts an important inhibitory effect on currents through recombinant $Ca_V1.3$ channels heterologously expressed in HEK-293 cells. This inhibition was specific given that δ co-expression did not affect endogenous K^+ current or heterologously expressed low threshold T-type channels (of the $Ca_V3.2$ class), and was not mimicked by the unrelated protein CD8. An exciting issue to be clarified relates to cell pathway(s) by which this inhibition occurs. Based on our findings we could speculate that distinct mechanisms underlie the decrease in current density after δ co-expression. It has been reported that the expression of short variants of the $Ca_V2\alpha_1$ subunit as well as the over-expression of the neuronal γ_2 subunit (stargazing) suppress currents through the activation of an endoplasmic reticulum resident RNA-dependent kinase (PERK) which activates components of the unfolded protein response (UPR) [50,51]. We therefore tested whether $Ca_V1.3$ current suppression by δ involved activation of the UPR using two mutant constructs that have shown to prevent the activation of endogenous PERK [34] and therefore inhibit the UPR. With the PERK ΔC and the K618A mutation the suppressive effect of δ remained unaltered, suggesting that activation of PERK may not play a role in the effects of the regulatory subunit. Likewise, to analyze the possible participation of a $Ca_V1.3$ channel internalization/degradation-dependent mechanism after δ co-expression, a series of inhibitors was used. We tested chloroquine, filipin III and MG-132, but all internalization inhibitors failed to alter the inhibitory actions of δ as current reduction persisted after treatment. However, several alternative mechanisms could be anticipated to elucidate the δ-induced regulation of $Ca_V1.3$ channel functional expression including: (i) that interaction with δ strongly affects the folding of nascent $Ca_V1.3\alpha_1$ subunits and affects the interaction with the $Ca_V\alpha_2\delta$ and/or $Ca_V\beta$ subunits, (ii) that δ is able to unmask retention signals that prevent the unassembled channel subunits from leaving the ER, and (iii) that δ over-expression could be increasing the degradation rate of the mRNAs for other Ca_V subunit reducing the channel protein levels and hence altering the functional expression of the channels.

Last, the expression and functional integrity of the $Ca_V\alpha_2\delta$-1 subunit in our model system was also confirmed pharmacologically by examining the chronic effects of GBP (1 mM) and AdGABA (1 mM) two anticonvulsant drugs that bind the auxiliary subunit [54,65]. GBP did not affect the amplitude of the currents and have a minor effect on the voltage dependence of activation. Exposure to the drug did, however, slow down the kinetics of inactivation. These results differ to that reported recently for recombinant neuronal Ca_V channels in which chronic incubation with GBP (1 mM) reduced currents through $Ca_V2.1\alpha_1/Ca_V\beta_4/Ca_V\alpha_2\delta$-2 and $Ca_V2.2\alpha_1/Ca_V\beta_{1b}/Ca_V\alpha_2\delta$-1 channels and shifted the voltage dependence of steady-state inactivation to more positive potentials [30]. A possible explanation for this difference is that the affinity of GBP to the $Ca_V\alpha_2\delta$ subunit may be modulated by other subunits, and that the effects of the drug depend on the composition and environment of the channel. Likewise, we also found that chronic treatment with AdGABA significantly inhibited macroscopic currents through $Ca_V1.3\alpha_1/Ca_V\beta_3/Ca_V\alpha_2\delta$-1 channels. To our knowledge, the inhibitory effect of AdGABA on $Ca_V1.3$ channel functional expression, represents a previously uncharacterized action of this drug, and is in agreement with our previous report describing the synthesis and pharmacological profile of AdGABA [54], in which we found that it reduces the functional expression of neuronal recombinant channels of the $Ca_V2.2$ class.

Acknowledgements

Appendix A. Supplementary data

Supplementary data associated with this article can be found, in the online version, at doi:10.1016/j.ceca.2009.08.006.

References

[1] D. Lipscombe, T.D. Helton, W. Xu, L-type calcium channels: the low down, J. Neurophysiol. 92 (2004) 2633–2641.

[2] S.N. Yang, P.O. Berggren, The role of voltage-gated calcium channels in pancreatic β-cell physiology and pathophysiology, Endocr. Rev. 27 (2006) 621–676.

[3] L. Lacinova, Voltage-dependent calcium channels, Gen. Physiol. Biophys. 24 (Suppl. 1) (2005) 1–78.

[4] M.A. Rogawski, W. Loscher, The neurobiology of antiepileptic drugs for the treatment of nonepileptic conditions, Nat. Med. 10 (2004) 685–692.

[5] I. Splawski, K.W. Timothy, L.M. Sharpe, N. Decher, P. Kumar, R. Bloise, C. Napolitano, P.J. Schwartz, R.M. Joseph, K. Condouris, H. Tager-Flusberg, S.G. Priori, M.C. Sanguinetti, M.T. Keating, $Ca_V1.2$ calcium channel dysfunction causes a multisystem disorder including arrhythmia and autism, Cell 119 (2004) 19–31.

[6] M. Day, Z. Wang, J. Ding, X. An, C.A. Ingham, A.F. Shering, D. Wokosin, E. Ilijic, Z. Sun, A.R. Sampson, E. Mugnaini, A.Y. Deutch, S.R. Sesack, G.W. Arbuthnott, D.J. Surmeier, Selective elimination of glutamatergic synapses on striatopallidal neurons in Parkinson disease models, Nat. Neurosci. 9 (2006) 251–259.

[7] J.F. Krey, R.E. Dolmetsch, Molecular mechanisms of autism: a possible role for Ca^{2+} signaling, Curr. Opin. Neurobiol. 17 (2007) 112–119.

[8] J. Surmeier, Calcium, ageing, and neuronal vulnerability in Parkinson's disease, Lancet Neurol. 6 (2007) 933–938.

[9] H. Bito, K. Deisseroth, R.W. Tsien, CREB phosphorylation and dephosphorylation: a Ca^{2+}- and stimulus duration-dependent switch for hippocampal gene expression, Cell 87 (1996) 1203–1214.

[10] R.E. Dolmetsch, U. Pajvani, K. Fife, J.M. Spotts, M.E. Greenberg, Signaling to the nucleus by an L-type calcium channel-calmodulin complex through the MAP kinase pathway, Science 294 (2001) 333–339.

[11] I.A. Graef, P.G. Mermelstein, K. Stankunas, J.R. Neilson, K. Deisseroth, R.W. Tsien, G.R. Crabtree, L-type calcium channels and GSK-3 regulate the activity of NF-ATc4 in hippocampal neurons, Nature 401 (1999) 703–708.

[12] X. Zhang, D.T. Odom, S.H. Koo, M.D. Conkright, G. Canettieri, J. Best, H. Chen, R. Jenner, E. Herbolsheimer, E. Jacobsen, S. Kadam, J.R. Ecker, B. Emerson, J.B. Hogenesch, T. Unterman, R.A. Young, M. Montminy, Genome-wide analysis of cAMP-response element binding protein occupancy, phosphorylation, and target gene activation in human tissues, Proc. Natl. Acad. Sci. U.S.A. 102 (2005) 4459–4464.

[13] H. Zhang, A. Maximov, Y. Fu, F. Xu, T.S. Tang, T. Tkatch, D.J. Surmeier, I. Bezprozvanny, Association of $Ca_V1.3$ L-type calcium channels with Shank, J. Neurosci. 25 (2005) 1037G–1049G.

[14] S.L. Johnson, W. Marcotti, Biophysical properties of $Ca_V1.3$ calcium channels in gerbil inner hair cells, J. Physiol. 586 (2008) 1029–1042.

[15] Z. Zhang, Y. Xu, H. Song, J. Rodriguez, D. Tuteja, Y. Namkung, H.S. Shin, N. Chiamvimonvat, Functional roles of $Ca_V1.3$ (α_{1D}) calcium channel in sinoatrial nodes: insight gained using gene-targeted null mutant mice, Circ. Res. 90 (2002) 981–987.

[16] A. Marcantoni, P. Baldelli, J.M. Hernandez-Guijo, V. Comunanza, V. Carabelli, E. Carbone, L-type calcium channels in adrenal chromaffin cells: role in pacemaking and secretion, Cell Calcium 42 (2007) 397–408.

[17] Y. Liang, S.J. Tavalin, Auxiliary β subunits differentially determine PKA utilization of distinct regulatory sites on $Ca_V1.3$ L type Ca^{2+} channels, Channels (Austin) 1 (2007) 102–112.

[18] M.L. Roberts-Crowley, A.R. Rittenhouse, Arachidonic acid inhibition of L-type calcium ($Ca_V1.3b$) channels varies with accessory $Ca_V\beta$ subunits, J. Gen. Physiol. 133 (2009) 387–403.

[19] D. Singer, M. Biel, I. Lotan, V. Flockerzi, F. Hofmann, N. Dascal, The roles of the subunits in the function of the calcium channel, Science 253 (1991) 1553–1557.

[20] K. Itagaki, W.J. Koch, I. Bodi, U. Klöckner, D.F. Slish, A. Schwartz, Native-type DHP-sensitive calcium channel currents are produced by cloned rat aortic smooth muscle and cardiac α_1 subunits expressed in Xenopus laevis oocytes and are regulated by α_2- and β-subunits, FEBS Lett. 297 (1992) 221–225.

[21] B. Welling, E. Bosse, A. Cavalie, R. Bottlender, A. Ludwig, W. Nastainczyk, V. Flockerzi, F. Hofmann, Stable co-expression of calcium channel α_1, β and α_2/δ subunits in a somatic cell line, J. Physiol. 471 (1993) 749–765.

[22] R. Felix, C.A. Gurnett, M. De Waard, K.P. Campbell, Dissection of functional domains of the voltage-dependent Ca^{2+} channel $\alpha_2\delta$ subunit, J. Neurosci. 17 (1997) 6884–6891.

[23] N. Qin, R. Olcese, E. Stefani, L. Birnbaumer, Modulation of human neuronal α_{1E}-type calcium channel by $\alpha_2\delta$-subunit, Am. J. Physiol. 274 (1998) C1324–C1331.

[24] N. Klugbauer, L. Lacinova, E. Marais, M. Hobom, F. Hofmann, Molecular diversity of the calcium channel $\alpha_2\delta$ subunit, J. Neurosci. 19 (1999) 684–691.

[25] T. Yasuda, L. Chen, W. Barr, J.E. McRory, R.J. Lewis, D.J. Adams, G.W. Zamponi, Auxiliary subunit regulation of high-voltage activated calcium channels expressed in mammalian cells, Eur. J. Neurosci. 20 (2004) 1–13.

[26] C. Canti, M. Nieto-Rostro, I. Foucault, F. Heblich, J. Wratten, M.W. Richards, J. Hendrich, L. Douglas, K.M. Page, A. Davies, A.C. Dolphin, The metal-ion-dependent adhesion site in the Von Willebrand factor-A domain of $\alpha_2\delta$ subunits is key to trafficking voltage-gated Ca^{2+} channels, Proc. Natl. Acad. Sci. U.S.A. 102 (2005) 11230–11235.

[27] A. Andrade, A. Sandoval, N. Oviedo, M. De Waard, D. Elias, R. Felix, Proteolytic cleavage of the voltage-gated Ca^{2+} channel $\alpha_2\delta$ subunit: structural and functional features, Eur. J. Neurosci. 25 (2007) 1705–1710.

[28] K. Dickman, P.T. Kurshan, T.L. Schwarz, Mutations in a Drosophila $\alpha_2\delta$ voltage-gated calcium channel subunit reveal a crucial synaptic function, J. Neurosci. 28 (2008) 31–38.

[29] P. Tuluc, G. Kern, G.J. Obermair, B.E. Flucher, Computer modeling of siRNA knockdown effects indicates an essential role of the Ca^{2+} channel $\alpha_2\delta$-1 subunit in cardiac excitation–contraction coupling, Proc. Natl. Acad. Sci. U.S.A. 104 (2007) 11091–11096.

[30] J. Hendrich, A.T. Van Minh, F. Heblich, M. Nieto-Rostro, K. Watschinger, J. Striessnig, J. Wratten, A. Davies, A.C. Dolphin, Pharmacological disruption of calcium channel trafficking by the $\alpha_2\delta$ ligand gabapentin, Proc. Natl. Acad. Sci. U.S.A. 105 (2008) 3628–3633.

[31] T.D. Helton, W. Xu, D. Lipscombe, Neuronal L-type calcium channels open quickly and are inhibited slowly, J. Neurosci. 25 (2005) 10247–11051.

[32] M. Mishina, T. Kurosaki, T. Tobimatsu, Y. Morimoto, M. Noda, T. Yamamoto, M. Terao, J. Lindstrom, T. Takahashi, M. Kuno, S. Numa, Expression of functional acetylcholine receptor from cloned cDNAs, Nature 307 (1984) 604–608.

[33] A. Sandoval, N. Oviedo, A. Andrade, R. Felix, Glycosylation of asparagines 136 and 184 is necessary for the $\alpha_2\delta$ subunit-mediated regulation of voltage-gated Ca^{2+} channels, FEBS Lett. 576 (2004) 21–26.

[34] H.P. Harding, Y. Zhang, D. Ron, Protein translation and folding are coupled by an endoplasmic-reticulum-resident kinase, Nature 397 (1999) 271–274.

[35] L.L. Cribbs, J.H. Lee, J. Yang, J. Satin, Y. Zhang, A. Daud, J. Barclay, M.P. Williamson, M. Fox, M. Rees, E. Perez-Reyes, Cloning and characterization of α_{1H} from human heart, a member of the T-type Ca^{2+} channel gene family, Circ. Res. 83 (1998) 103–109.

[36] T. Avila, A. Andrade, R. Felix, Transforming growth factor-β1 and bone morphogenetic protein-2 downregulate $Ca_V3.1$ channel expression in mouse C2C12 myoblasts, J. Cell. Physiol. 209 (2006) 448–456.

[37] O.P. Hamill, A. Marty, E. Neher, B. Sakmann, F.J. Sigworth, Improved patch-clamp techniques for high resolution current recording from cells and cell-free membrane patches, Pflugers Arch. 391 (1981) 85–100.

[38] G. Avila, A. Sandoval, R. Felix, Intramembrane charge movement associated with endogenous K^+ channel activity in HEK-293 cells, Cell. Mol. Neurobiol. 24 (2004) 317–330.

[39] C.A. Gurnett, R. Felix, K.P. Campbell, Extracellular interaction of the voltage-dependent Ca^{2+} channel $\alpha_2\delta$ and α_1 subunits, J. Biol. Chem. 272 (1997) 18508–18512.

[40] A. Andrade, M.B. de Leon, O. Hernandez-Hernandez, B. Cisneros, R. Felix, Myotonic dystrophy CTG repeat expansion alters Ca^{2+} channel functional expression in PC12 cells, FEBS Lett. 581 (2007) 4430–4438.

[41] A. Scholze, T.D. Plant, A.C. Dolphin, B. Nürnberg, Functional expression and characterization of a voltage-gated $Ca_V1.3_{(\alpha 1D)}$ calcium channel subunit from an insulin-secreting cell line, Mol. Endocrinol. 15 (2001) 1211–1221.

[42] A. Singh, M. Gebhart, R. Fritsch, M.J. Sinnegger-Brauns, C. Poggiani, J.C. Hoda, J. Engel, C. Romanin, J. Striessnig, A. Koschak, Modulation of voltage- and Ca^{2+}-dependent gating of $Ca_V1.3$ L-type calcium channels by alternative splicing of a C-terminal regulatory domain, J. Biol. Chem. 283 (2008) 20733–20744.

[43] W. Xu, D. Lipscombe, Neuronal $Ca_V1.3_{\alpha 1}$ L-type channels activate at relatively hyperpolarized membrane potentials and are incompletely inhibited by dihydropyridines, J. Neurosci. 21 (2001) 5944–5951.

[44] P.S. Yang, B.A. Alseikhan, H. Hiel, L. Grant, M.X. Mori, W. Yang, P.A. Fuchs, D.T. Yue, Switching of Ca^{2+}-dependent inactivation of $Ca_V1.3$ channels by calcium binding proteins of auditory hair cells, J. Neurosci. 26 (2006) 10677–10689.

[45] J.P. Imredy, D.T. Yue, Mechanism of Ca^{2+}-sensitive inactivation of L-type Ca^{2+} channels, Neuron 12 (1994) 1301–1318.

[46] M. de Leon, Y. Wang, L. Jones, E. Perez-Reyes, X. Wei, T.W. Soong, T.P. Snutch, D.T. Yue, Essential Ca^{2+}-binding motif for Ca^{2+}-sensitive inactivation of L-type Ca^{2+} channels, Science 270 (1995) 1502–1506.

[47] W.A. Catterall, Structure and regulation of voltage-gated Ca^{2+} channels, Annu. Rev. Cell. Dev. Biol. 16 (2000) 521–555.

[48] C.A. Gurnett, M. De Waard, K.P. Campbell, Dual function of the voltage-dependent Ca^{2+} channel $\alpha_2\delta$ subunit in current stimulation and subunit interaction, Neuron 16 (1996) 431–440.

[49] A. Raghib, F. Bertaso, A. Davies, K.M. Page, A. Meir, Y. Bogdanov, A.C. Dolphin, Dominant-negative synthesis suppression of voltage-gated calcium channel Ca$_V$2.2 induced by truncated constructs, J. Neurosci. 21 (2001) 8495–8504.

[50] K.M. Page, F. Heblich, A. Davies, A.J. Butcher, J. Leroy, F. Bertaso, W.S. Pratt, A.C. Dolphin, Dominant-negative calcium channel suppression by truncated constructs involves a kinase implicated in the unfolded protein response, J. Neurosci. 24 (2004) 5400–5409.

[51] A. Sandoval, A. Andrade, A.M. Beedle, K.P. Campbell, R. Felix, Inhibition of recombinant N-type Ca$_V$ channels by the γ_2 subunit involves unfolded protein response (UPR)-dependent and UPR-independent mechanisms, J. Neurosci. 27 (2007) 3317–3327.

[52] F.J. Moss, A.C. Dolphin, J.J. Clare, Human neuronal stargazin-like proteins, γ_2, γ_3 and γ_4; an investigation of their specific localization in human brain and their influence on Ca$_V$2. 1 voltage-dependent calcium channels expressed in *Xenopus oocytes*, BMC Neurosci. 4 (2003) 23.

[53] A. Vega-Hernandez, R. Felix, Down-regulation of N-type voltage-activated Ca^{2+} channels by gabapentin, Cell. Mol. Neurobiol. 22 (2002) 185–190.

[54] G. Zoidis, I. Papanastasiou, I. Dotsikas, A. Sandoval, R.G. Dos Santos, Z. Papadopoulou-Daifoti, A. Vamvakides, N. Kolocouris, R. Felix, The novel GABA adamantane derivative (AdGABA): design, synthesis, and activity relationship with gabapentin, Bioorg. Med. Chem. 13 (2005) 2791–2798.

[55] P.M. Mich, W.A. Horne, Alternative splicing of the Ca^{2+} channel β_4 subunit confers gabapentin specificity for inhibition of Ca$_V$2.1 trafficking, Mol. Pharmacol. 74 (2008) 904–912.

[56] M.J. Field, P.J. Cox, E. Stott, H. Melrose, J. Offord, T.Z. Su, S. Bramwell, L. Corradini, S. England, J. Winks, R.A. Kinloch, J. Hendrich, A.C. Dolphin, T. Webb, D. Williams, Identification of the $\alpha_2\delta$-1 subunit of voltage-dependent calcium channels as a molecular target for pain mediating the analgesic actions of pregabalin, Proc. Natl. Acad. Sci. U.S.A. 103 (2006) 17537–17542.

[57] M.G. Kang, R. Felix, K.P. Campbell, Long-term regulation of voltage-gated Ca^{2+} channels by gabapentin, FEBS Lett. 528 (2002) 177–182.

[58] P. Safa, J. Boulter, T.G. Hales, Functional properties of Cav1.3 (α_{1D}) L-type Ca^{2+} channel splice variants expressed by rat brain and neuroendocrine GH$_3$ cells, J. Biol. Chem. 276 (2001) 38727–38737.

[59] M. De Waard, K.P. Campbell, Subunit regulation of the neuronal α_{1A} Ca^{2+} channel expressed in *Xenopus oocytes*, J. Physiol. 485 (1995) 619–634.

[60] L. Parent, T. Schneider, C.P. Moore, D. Talwar, Subunit regulation of the human brain α_{1E} calcium channel, J. Membr. Biol. 160 (1997) 127–140.

[61] E. Shistik, T. Ivanina, T. Puri, M. Hosey, N. Dascal, Ca^{2+} current enhancement by α_2/δ and β subunits in *Xenopus oocytes*: contribution of changes in channel gating and α_1 protein level, J. Physiol. 489 (1995) 55–62.

[62] R. Bangalore, G. Mehrke, K. Gingrich, F. Hofmann, R.S. Kass, Influence of L-type Ca channel α_2/δ-subunit on ionic and gating current in transiently transfected HEK-293 cells, Am. J. Physiol. 270 (1996) H1521–H1528.

[63] G.A. Fuller-Bicer, G. Varadi, S.E. Koch, M. Ishii, I. Bodi, N. Kadeer, J.N. Muth, G. Mikala, N.N. Petrashevskaya, M.A. Jordan, S.P. Zhang, N. Qin, C.M. Flores, I. Isaacsohn, M. Varadi, Y. Mori, W.K. Jones, A. Schwartz, Targeted disruption of the voltage-dependent calcium channel α_2/δ-1-subunit, Am. J. Physiol. Heart Circ. Physiol. 297 (2009) H117–H124.

[64] M.E. Williams, D.H. Feldman, A.F. McCue, R. Brenner, G. Velicelebi, S.B. Ellis, M.M. Harpold, Structure and functional expression of α_1, α_2, and β subunits of a novel human neuronal calcium channel subtype, Neuron 8 (1992) 71–84.

[65] N.S. Gee, J.P. Brown, V.U. Dissanayake, J. Offord, R. Thurlow, G.N. Woodruff, The novel anticonvulsant drug, gabapentin (Neurontin), binds to the $\alpha_2\delta$ subunit of a calcium channel, J. Biol. Chem. 271 (1996) 5768–5776.

Appendix A. Supplementary data
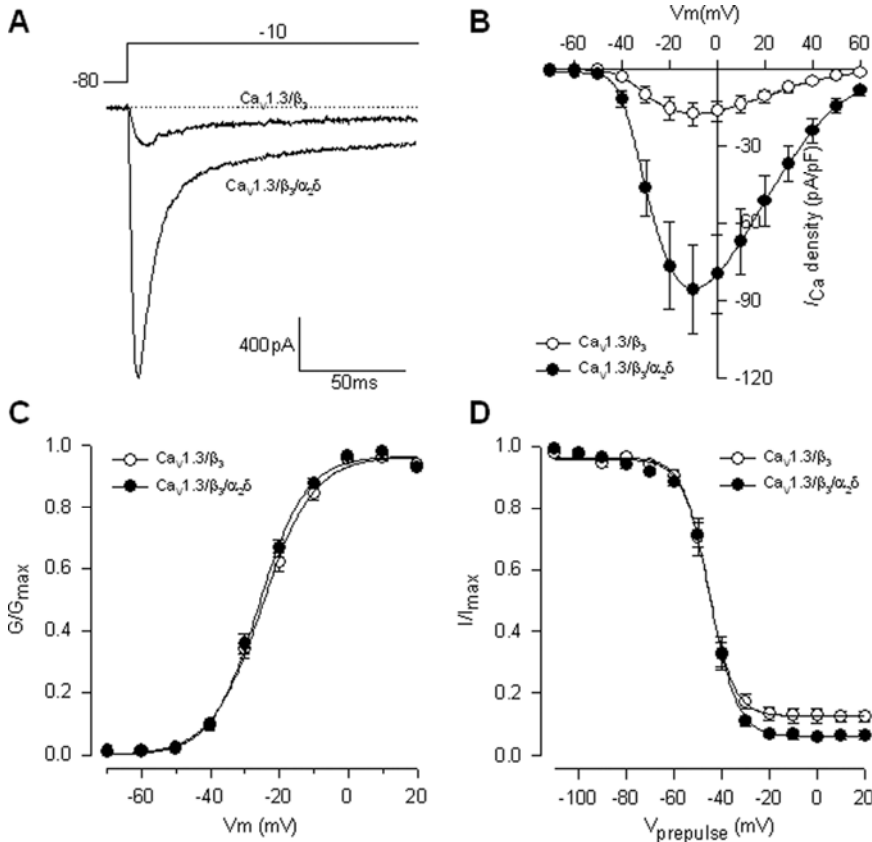
Supplementary Fig. S1. Ca^{2+}-dependent inactivation and $Ca_V\alpha_2\delta$-1 subunit regulation of currents through recombinant $Ca_V1.3$ channels. (A) Representative traces of Ca^{2+} macroscopic current (I_{Ca}) recorded from HEK-293 cells expressing $Ca_V1.3\alpha_1/\beta_3$ channels in absence and presence of $\alpha_2\delta$-1, using solutions B and D (Table 1). Currents were elicited by a 140 ms depolarizing pulse to -10 mV from a V_h of -80 mV. (B) Average I–V relationships for I_{Ca} recorded from HEK-293 transfected as in A. (C) Voltage dependence of activation of recombinant $Ca_V1.3\alpha_1/\beta_3$ channels in absence and presence of the $Ca_V\alpha_2\delta$-1 subunit. G–V curves were plotted by converting peak current values of panel B to peak conductance values using Eq. (1), and the mean data were fitted with a Boltzmann function (Eq. (2)). $n = 10$ cells. (D) Voltage dependence of steady-state inactivation of recombinant $Ca_V1.3\alpha_1/\beta_3$ channels with or without $Ca_V\alpha_2\delta$-1. Currents were elicited by 2 s conditioning pulses from a V_h of -80 mV in 10 mV steps from -110 to $+20$ mV. Data were plotted against the conditioning pulse, and were fitted with a Boltzmann function (Eq. (3)). $n = 14$ recorded cells.
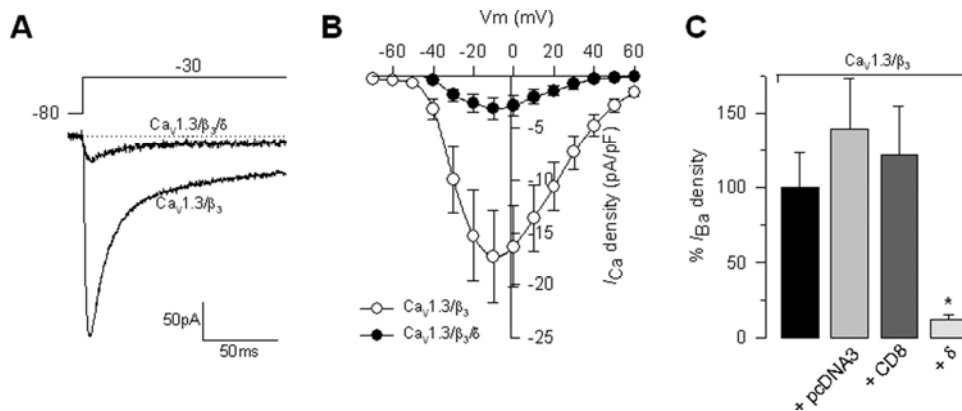
Supplementary Fig. S2. The δ subunit inhibits the functional expression of $Ca_V1.3\alpha_1/\beta_3$ channels. (A) Representative traces of I_{Ca} recorded from HEK-293 cells transfected with the $Ca_V1.3\alpha_1/\beta_3$ cDNAs in absence and presence of δ, using solutions B and D (Table 1). Currents were elicited as in A. (B) Average *I–V* relationships for I_{Ca} recorded in cells expressing the $Ca_V1.3\alpha_1/\beta_3$ channels with or without the δ subunit. (C) Relative I_{Ca} densities obtained from cells that expressed the recombinant $Ca_V1.3\alpha_1/\beta_3$ channels alone (control; solid bar), plus the empty vector pcDNA3, the transmembrane protein CD8 or the δ subunit ($n = 10$–14 cells). The asterisk denotes a significant difference with respect to the control ($p < 0.05$).
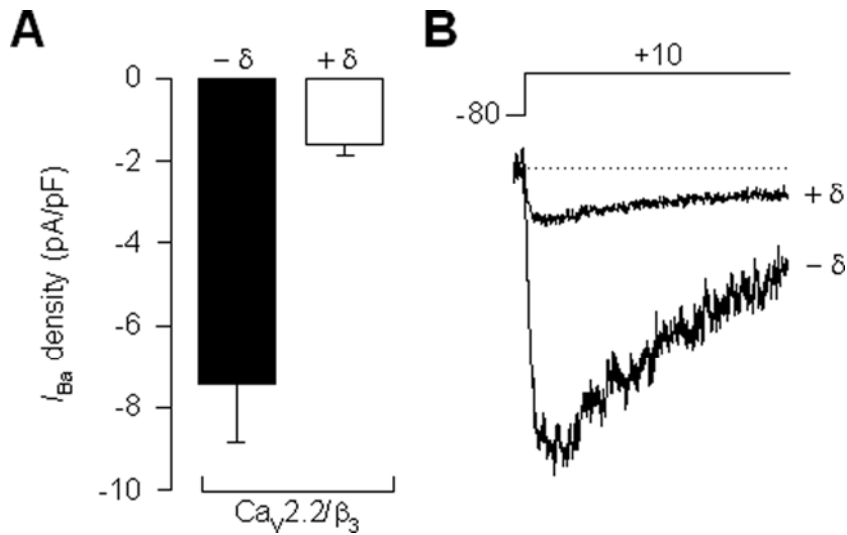
Supplementary Fig. S3. The $Ca_V\delta$ domain inhibit current through $Ca_V2.2/Ca_V\beta_3$ channels heterologously expressed in HEK-293 cells. (A) Comparison of I_{Ba} density in individual HEK-293 cells determined as the current amplitude at V_m of +10 mV normalized by cell capacitance (pA/pF). (B) Representative current traces from control cells ($-\delta$) or cells co-expressing $Ca_V\delta$ ($+\delta$) using recording solutions A and D ([Table 1](#)). Currents were elicited by voltage steps to +10 mV from a V_h of −80 mV.
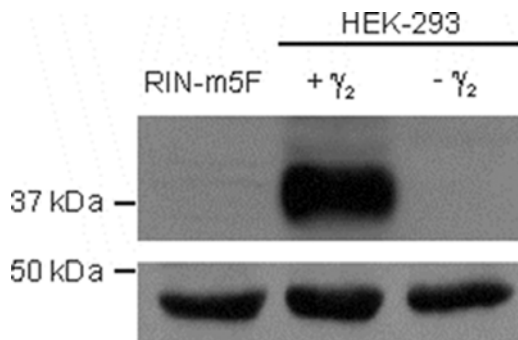
Supplementary Fig. S4. The $Ca_V\gamma$ subunit is not expressed in the RIN-m5F cells. Aliquots (40 µg) of protein extract from RIN-m5F cells or HEK-293 cells (untransfected or transiently transfected with the $Ca_V\gamma_2$ subunit) were electrophoresed on a 10% SDS-polyacrylamide gel and proteins were then transferred to nitrocellulose. Membranes were blocked for 1–2 h in TBST (100 mM Tris–HCl pH 8.0, 150 mM NaCl, 0.5% (v/v) Tween-20) with 5% (w/v) low-fat dried milk and then incubated overnight at 4 °C with a rabbit polyclonal antibody against $Ca_V\gamma_2$ subunit. Specific proteins were visualized by using the enhanced chemiluminescence (ECL) Western blotting kit (Amersham Life Science) according to the manufacturer's instructions. As a protein loading control, membranes were striped and incubated with a mouse monoclonal anti-β-actin antibody (lower panel).